J. Chem. Soc. Nigeria, Vol. 49, No. 3, pp 327- 341 [2024]

REMOVAL OF AN ORGANIC DYE FROM TURMERIC (*CURCUMA LONGA*) USING ACTIVATED CARBON PREPARED FROM GROUNDNUT (*ARACHIS HYPOGEA*) HUSK

I. Orji *[1], A. Njoku Eke-Anyanwu [1]

[1] Department of Pure and Industrial Chemistry, University of Port Harcourt, Nigeria

*Corresponding Author: ikodiya.orji@uniport.edu.ng; +234 8104927314

ABSTRACT

Carbon-based adsorbents were prepared from groundnut husk by impregnation with H_3PO_4 and NaOH before or after carbonization. The adsorbents were characterised by Brunauer-Emmett-Teller (BET) adsorption/desorption isotherms, scanning electron microscopy (SEM), thermogravimetric/differential thermal analysis (TGA/DTA), and Fourier-Transform infrared spectroscopy (FTIR). These adsorbents were used for the removal of a turmeric based organic dye from aqueous solution. The results obtained from measuring the pH, temperature, and particle size effects on the adsorption process showed that the adsorbent impregnated with H_3PO_4 before carbonization (CA-B), achieved a higher percentage removal of turmeric dye at all parameters studied. The pseudo-second-order kinetic model explained the experimental data, the adsorption was controlled by liquid film and intraparticle diffusion models simultaneously, the equilibrium data was a good fit to the Langmuir adsorption isotherm model, and physisorption was the predominant sorption process. The results from this research have shown that adsorbents with suitable characteristics for the removal of turmeric dye from aqueous solution could be produced from groundnut husk.

Keywords: Adsorbents, Turmeric, Curcumin, Activated Carbon, Groundnut Husk.

INTRODUCTION

The bright yellow or orange colour in turmeric derived from the *Curcuma longa* plant, is mainly due to the presence of three major pigments collectively known as curcuminoids. These pigments are: curcumin, also known as diferuloylmethane, demethoxy-curcumin, otherwise known as p-hydroxycinnamoylferuloylmethane, and bisdemethoxycurcumin also known as p,p-dihydroxydicinnamoylmethane [1]. Turmeric has been used for centuries as a spice, food colouring agent and dietary supplement [2]. Beyond this traditional use, it is used for the manufacture of dyes for textile, perfume, hair, cosmetics and soap industries [1, 3-5]. Research has shown that turmeric contains between 25 to 70 % carbohydrates [6], making it a good raw material for starch manufacture [7-9]. Because of the presence of the π to π star conjugated electron system in the structure of the curcuminoids (Figure 1), turmeric has gained significant attention due to its potential as a source of natural dye for applications in photonics. Research into the application of turmeric in dye-sensitized solar cell (DSSC), nonlinear optics, tuneable dye lasers, dyes for organic light emitting diodes (OLEDs), and dye-sensitized optical data storage which gained traction in recent years is ongoing

ISSN 0795 - 22066

[1, 10-14]. It is expected that advancements in this area of research involving an integration of materials science and organic chemistry would lead to its practical implementation in large scale application of this nature in the nearest future. Consequent on these traditional and emerging applications of turmeric and curcumin-based pigments in industry, there is bound to be an increase in the generation of curcumin-contaminated waste streams for discharge into our waterways. Curcumin is a natural dye which means it is more degradable relative to synthetic dyes, however, when the concentration of curcumin which enters wastewater or effluent is beyond the recommended allowed unit, it can have several undesirable effects on the environment and water treatment processes, hence the need to remove them from industrial runoffs before discharge into our water ways in order to mitigate some of these negative environmental impacts.

Groundnut husks are a potential source of activated carbon (AC) due to their high carbon content and porous nature [15]. Preparing AC from groundnut husk is an environmentally friendly alternative to sources like wood, coal and lignite [16] which have many other industrial and domestic applications, as it utilizes a cheap, easily available, and renewable agricultural waste product for the preparation of cost-effective adsorbents for treating industrial effluents, through a simple method of activation and carbonization. To this end, several researchers have utilized groundnut husks as precursors for preparation of ACs with promising results [14,15,17-20]. While Nigeria is not one of the major global producers of turmeric, the reverse is the case for groundnut production. The major groundnut-producing states of Nigeria like Kano, Adamawa, Katsina, and Gombe have fertile soils and favourable growing conditions for groundnuts [21]. As a significant cash crop for many farmers in Nigeria, it serves as a source of income and employment [22]. The nuts are used for various purposes, including direct consumption, oil extraction, and processing into products like groundnut paste, groundnut cake, groundnut flour, and for export [23]. Thus, a considerable volume of groundnut husk waste is generated annually in these regions. The conversion of these husks into value added products like AC for effluent treatment could drive cultivation of groundnut and further increase the revenue base of the local farmers, while improving our waterways.

This work was carried out to investigate the removal of an organic dye from *Curcuma longa* using activated carbon from *Arachis hypogea* husk.

MATERIALS AND METHODS

Raw groundnut husks and turmeric rhizomes used in this research were obtained from a local market in Port Harcourt, Nigeria. The husks were washed with distilled water and dried to constant weight at 110 ^{o}C. Two methods were adopted in the preparation process using analytical grades of phosphoric acid (H_3PO_4) and sodium hydroxide (NaOH).

Preparation of Adsorbents: In the first method, the groundnut husks were activated by soaking them for 24 hours in a 30% solution of the

ISSN 0795 - 22066

activating agent (H_3PO_4 and NaOH), at a mass to volume ratio of 3:10 (groundnut husk:activating agent solution), after which it was filtered, dried, carbonized at 400 ^oC and pulverized. These samples were labelled as acid activated before carbonization (ABC-ACID) and base activated before carbonization (ABC-BASE). In the second route, the groundnut husks were carbonized at the same temperature before soaking in the activating agents for the same duration under the same concentration of activating agent, and mass to volume ratio. These were labelled as carbonized before activation with an acid (CBA-ACID), and carbonized before activation with a base (CBA-BASE). The unactivated carbonized raw groundnut husk (CRGH) was left as a control.

Characterization of Adsorbents: The textural properties of the AC samples were examined using N_2 adsorption at 77k on (Quarterchrome Instruments). The samples were degassed under vacuum at 250 ^oC, and the Brunauer-Emmett-Teller (BET) surface areas calculated from the desorption data. The pore characteristics (volume and diameter) were also obtained using the BJH method. Surface structures and temperature stability of the adsorbents were studied using scanning electron microscopy (SEM) (PRO:X:800-07334, Phenom World) and thermogravimetric /differential thermal analysis (TGA/DTA) (PerkinElmer Thermal) respectively. The differences in the absorption peaks of the functional groups of all the adsorbent samples were confirmed with Fourier transform infrared (FTIR) spectroscopy, (Carg/y 630, Agilent Technology), in the range of 4000 – 400 cm^{-1}.

Dye: The turmeric rhizomes were peeled, cut into smaller pieces, and dried to constant weight in an oven at moderate heat (40 ^oC). The resultant dried, flaky, small-sized turmeric pieces were blended to yield a fine yellow powder which was immersed in cold distilled water (1:10; mass of turmeric : volume of distilled water), and allowed to stand for 48 hours before filtering to obtain the stock solution. The structures of the major colouring components of the dye extract and their common names are given in Figure 1.

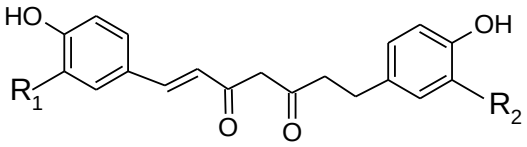

(a) $R_1 = R_2 = OCH_3$ = curcumin

(b) $R_1 = OCH_3$, $R_2 = H$ = demethoxy-curcumin

(c) $R_1 = R_2 = H$ = bisdemethoxycurcumin

Figure 1: Structure of the principal colouring components of curcumin

Adsorption Studies: A series of Batch adsorption assays were carried out using the activated carbon derived from groundnut husk in 100ml agitation bottles on a mechanical shaker (120 oscillations/min). The experiments were performed using 0.1 g of adsorbents taken in 30 ml of solution. The effect of pH, temperature and method of activation on the degree of colour removal was carried out by varying the pH from 2 to 12, temperature from 40 ^oC to 80 ^oC and

ISSN 0795 - 22066

particle size from 50 to 600 µm. The concentration of the dye solution before and after adsorption was measured with a UV spectrophotometer (Mettler Toledo) at a wavelength of 420nm (maximum wavelength of absorption of curcumin). All adsorptions were carried out in triplicates and the average value used for the calculation of the equilibrium adsorption capacity, q_e, the adsorption capacity at different time intervals, q_t, and the percentage of dye removed were calculated using equations 1, 2, and 3 respectively.

$$q_e = \frac{V(C_o - C_e)}{m} \quad (1)$$

$$q_t = \frac{V(C_o - C_t)}{m} \quad (2)$$

$$\% \text{ Dye Removal} = \frac{(C_o - C_e) \times 100}{C_o} \quad (3)$$

Where C_o denotes the initial concentration of the dye, C_e is the equilibrium concentration of the dye, C_t is the concentration of the dye at any given time t, m is the mass of adsorbent, and V is the volume of the dye solution.

Kinetic and Equilibrium Data: The adsorption kinetics for the colour removal was determined by fitting the experimental data obtained from the best performing adsorbent (ABC-ACID), into the pseudo - first order, pseudo – second order and Elovich kinetic models. The linear forms of these models are shown in equations 4, 5 and 6 respectively.

$$\ln(q_e - q_t) = \ln(q_e) - K_1 \times t \quad (4)$$

$$\frac{t}{q_t} = \left(\frac{1}{k_2 (q_e)^2}\right) + \frac{t}{q_e} \quad (5)$$

$$q_t = \frac{\ln (a+b)}{b} + \frac{\ln t}{b} \quad (6)$$

The diffusion mechanism governing the sorption process was investigated using the liquid film diffusion and intraparticle diffusion models, the linear forms of which are shown as equations 7 and 8 below.

$$\ln(1 - q_t/q_e) = -K_{fd}t + C \quad (7)$$

$$q_t = K_{int}t_{1/2} + C \quad (8)$$

Where K_{fd} is the film diffusion rate constant, and K_{int} is the intraparticle diffusion rate constant. If the plot of $-\ln(1 - q_t/q_e)$ against t gives a straight line with a zero intercept, this would indicate that the sorption process is controlled by diffusion through the liquid film surrounding the adsorbent. If, however, a plot of q_t versus $t_{1/2}$ gives rise to a straight line which passes through the origin, with a slope of K_{int}, then intraparticle diffusion is the only mechanism for the sorption process.

The sorption isotherms were simulated using Freundlich, Langmiur, Temkin, and Dubinin–Radushkevich isotherms. The Langmuir isotherm assumes a monolayer adsorption process on a homogeneous surface with no interaction between adsorbed molecules, and the Freundlich isotherm, on the other hand, assumes a multilayer adsorption process with heterogeneous adsorption sites and provides information about the adsorption intensity [24].

With linearized isotherms as presented in equations 9 to 12.

$$\ln q_e = \ln K_F + \frac{1}{n}\ln C_e \quad (9)$$

$$\frac{C_e}{q_e} = \frac{1}{X_m K_L b} + \frac{C_e}{X_m} \quad (10)$$

$$q_e = \frac{RT}{b_T}\ln K_T + \frac{RT}{b_T}\ln C_e \quad (11)$$

$$q_e = \ln q_m - \beta\varepsilon^2 \quad (12)$$

ISSN 0795 - 22066

The main properties of the Langmuir isotherm may be described by a dimensionless constant (the separation factor), R_L. It is given by the following equation:

$$R_L = \frac{1}{1+ bC_0} \quad (13)$$

Where C_0 (mg/L) is the highest initial dye concentration, and the value of R_L postulates whether the isotherm is unfavourable (R_L >1), linear (R_L =1), favourable (0 < R_L <1), or irreversible (R_L =0)

K_F = Freundlich constant (mg/g)(mg L^{-1})

1/n = A measure of the surface heterogeneity, with values between 0 and 1

X_m = Maximum adsorption capacity upon complete coverage of the adsorption sites of the adsorbents (mg/g)

K_L = Langmuir constant (L mg^{-1})

K_T = Temkin constant

R = Gas constant (J mol–1 K–1)

T = Temperature (K)

b_T is related to the adsorption intensity (J/mol)

β = Activity coefficient related to the mean sorption energy E (kJ/mol)

E is calculated using Equation 14.

$$E = \frac{1}{(2\beta)^{1/2}} \quad (14)$$

ε = Polanyi potential, which is expressed by Equation 15.

$$\varepsilon = RT\ln\left(1 + \frac{1}{C_e}\right) \quad (15)$$

Table 1: Surface Characteristics of the Adsorbents

Characteristic	**ABC-ACID**	**ABC-BASE**	**CBA-ACID**	**CBA-BASE**	**CRGH**
BET surface area (m^2g^{-1})	352.49	336.44	213.80	213.60	167.33
Total pore volume ($cm^3\ g^{-1}$)	0.28	0.19	0.13	0.11	0.09
Average pore size (Å)	2.90	2.74	2.14	2.13	3.01

RESULTS AND DISCUSSION

Surface Characteristics of Adsorbents

BET: From the results of the BET analysis of the samples presented in Table 1, it can be seen that the surface areas of all the AC samples are higher than that of the unactivated carbonized raw groundnut husk (CRGH). The samples impregnated with the activating agents before carbonization exhibited higher surface areas relative to the samples carbonized before impregnation, and the samples activated after carbonization showed little difference in their surface areas. The same trend is observed in the total pore volume and average pore size values of all the samples, except in the average pore size of the control which is highest of all. But it does appear that the method of impregnation is more important to the surface property of the carbonaceous adsorbents than the identity of the activating agents. For instance, there was more than a 50% increase in the surface area of the ABC-ACID sample relative to that of the CRGH sample which was used as control. Conversely, only approximately 20% increase in the surface area of the CBA-ACID sample was achieved by

ISSN 0795 - 22066

the impregnation after carbonization with acid, thus the surface characteristics of the carbonized samples were improved by the activation process.

Table 1: Surface Characteristics of the Adsorbents

SEM: The AC sample CRGH which was not activated large sheets with flat, irregular smooth surface devoid of plenty pores or channels. This was reflected in the BET surface area, pore volume, and pore size values which were the lowest among the five adsorbents. This is in contrast with the non-uniform, rough surface of ABC – ACID, ABC-BASE, CBA – ACID, and CBA-BASE samples (Figure 3). The interconnected pores, cracks and channels developed as a result of activating the carbonaceous material with phosphoric acid and sodium hydroxide before or after carbonizing, are clearly seen on the scanning electron micrographs on display, especially that of sample ABC – ACID.

FTIR: It is important to identify the functional groups in order to understand the possible effect of the availability and reactivity of surface functional groups on the adsorption capacity of the adsorbent of interest. Consequently, the functional groups on the surface of the adsorbents were identified by FTIR. As shown in Figure 5, the CRGH sample didn't have an elaborate spectrum with absorption speaks corresponding to a lot of functional groups.

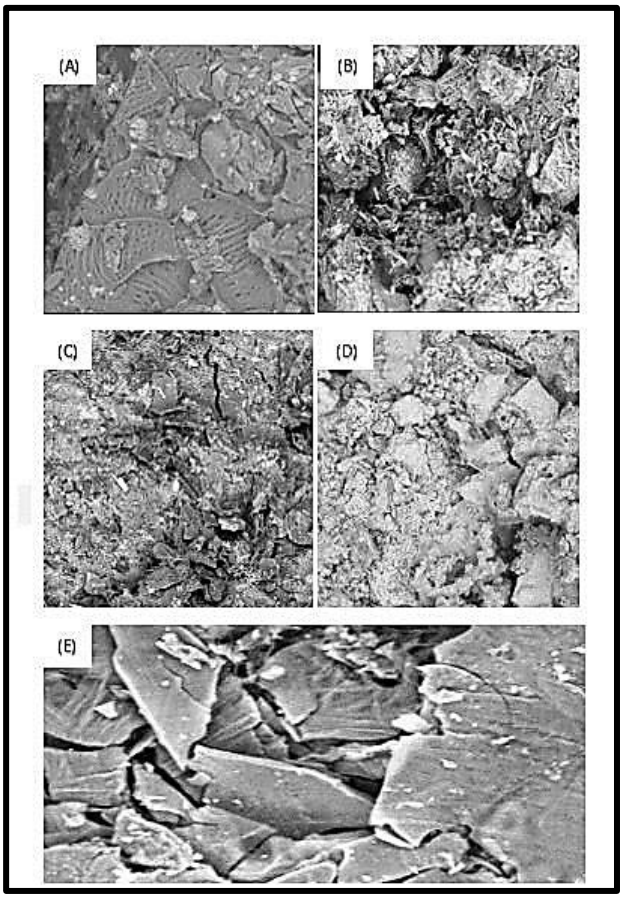

Figure 3: SEM Images of (A)ABC - ACID (B)ABC-BASE (C)CBA-ACID (D)CBA-BASE (E)CRGH

However, a close look at the spectra will show that several functional groups were either eliminated or enhanced in the activated adsorbents by the various treatment methods. For instance, the small absorption peak arising out of the O-H functional group in the CRGH sample at 3306.15 cm^{-1} was completely eliminated in the base activated samples of the AC, while this absorption peak was enhanced as seen at wavenumber 3246.51 cm^{-1} and 3231.60 cm^{-1} for CBA-BASE and ABC-BASE respectively. Thus, it appears that the acid treatment removed the OH functional group on the surface of the AC samples, but enhanced it in the base activated samples. In addition to this, the base activated

ISSN 0795 - 22066

samples showed absorption peaks attributable to -C=O functional groups, assigned to the - C=O bond of an inorganic carbonate which were conspicuously absent in the IR spectrum of the acid activated adsorbent samples.

These are in addition to other characteristic peaks indicating the presence of C-H aliphatic bending group appearing, C=C and C= C conjugated bonds, and alkane CH and CH_2 stretch aliphatic groups at approximately 1440 cm^{-1}, 2010 cm^{-1} and 2900 cm^{-1} respectively.

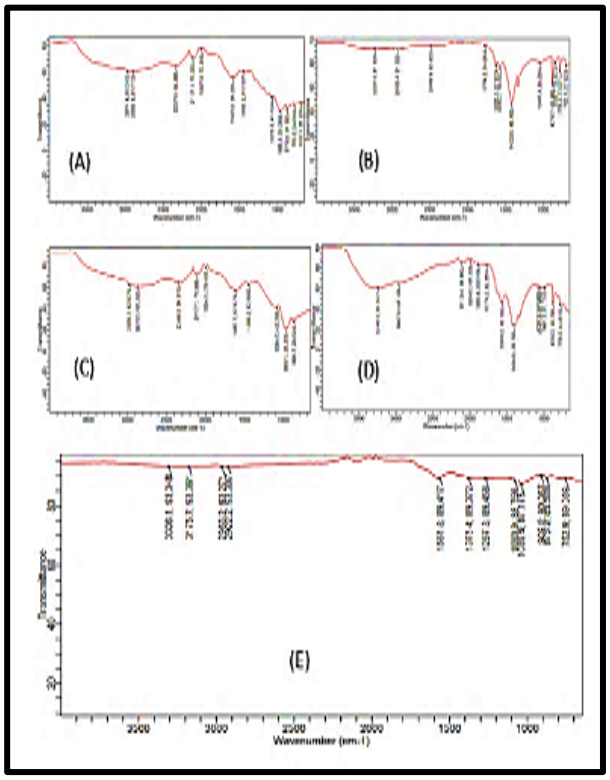

Figure 5: FTIR of (A) ABC - ACID (B) ABC-BASE (C) CBA-ACID (D)CBA-BASE (E) CRGH

Thermal analysis: Analysis of the thermal properties of the adsorbent used as control and the sample with the highest surface area (ABC – ACID) by combined TGA/DTA yielded the plot presented in Figure 4. The peaks detected on the DTA for both samples around 105 ^oC indicate the removal of water and other more volatile components on the surface of the adsorbents. It shows the 1st derivative peak temperature of decomposition to be 380 ^oC. The TGA for CRGH (Figure 4a) shows a multi - step decomposition with no stable intermediates, which could be due to instability of the intermediates [25], but there was higher mass loss between 250 to 550 ^oC.

The acid pre-treated carbonized adsorbent (ABC-ACID) also displays a multi-step decomposition and a derivative peak temperature (Tp) of 390 ^oC (Figure 4b). The relatively higher temperature stability of ABC-ACID demonstrated by the increase of the peak temperature from 380 ^oC in the unactivated sample, to 390 ^oC in the acid activated sample, is a confirmation that chemical modification of the surface of the samples was achieved.

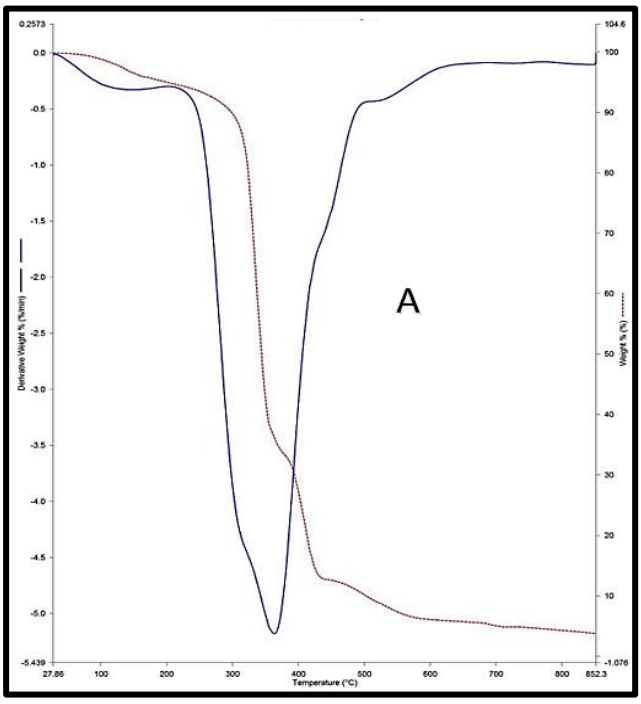

ISSN 0795 - 22066

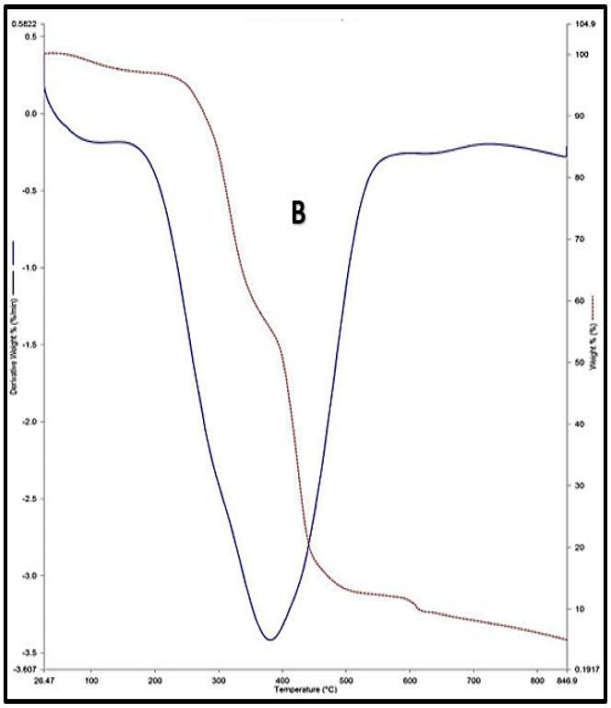

Figure 4: TGA curve of (A) CRGH (B) ABC – ACID

ADSORPTION STUDIES

Effect of pH, Temperature, Particle Size and Activation Method on the Adsorption Efficiency: The improved surface characteristics of the adsorbents by the various treatment protocols is shown by the enhanced adsorption capacities of the activated samples relative to the unactivated sample. The results obtained from investigating the effect of pH, temperature, particle size, and method of activation on the percentage adsorption of dye indicated that the pH of the dye solution played a significant role in the adsorption process, as did the temperature, since it was observed that the removal efficiency increased with decreasing pH values and increasing temperature (Figures 5, 6, and 7). The results however, show that the effect of pH on the adsorption capacity of the samples is more pronounced than that of the temperature since higher % removal was recorded for the pH dependent variable relative to the temperature. This is understandable because in neutral and acidic media, curcumin is deprotonated and exists in the keto form, while in basic media, the enol form predominates [1] (Nair, 2019). Since the solubility of curcumin is reduced in aqueous medium, the lower the pH, the less available it is in the solution, and the higher the removal capacity. Curcumin is a natural dye which is decomposed at high temperature, so increased temperature enhances the adsorption capacity.

The percentage dye removal is also affected by the particle size of the ACs, as indicated by the different percentage dye removal recorded for the different particle sizes. In all the samples, the 150 µm particle size recorded the highest degree of removal, while the 600 µm particle size recorded the lowest degree of dye removal. Generally, the samples activated before carbonizing showed higher removal efficiencies relative to the samples carbonized before activation, also the acid activated samples exhibited higher removal efficiencies than the base activated samples.

Sample ABC-ACID, which was activated with phosphoric acid before carbonization consistently showed the highest percentage adsorption relative to the other adsorbents. The trend of the removal follows the pattern, ABC-ACID >CBA-ACID > ABC-BASE > CBA-BASE > CRGH.

ISSN 0795 - 22066

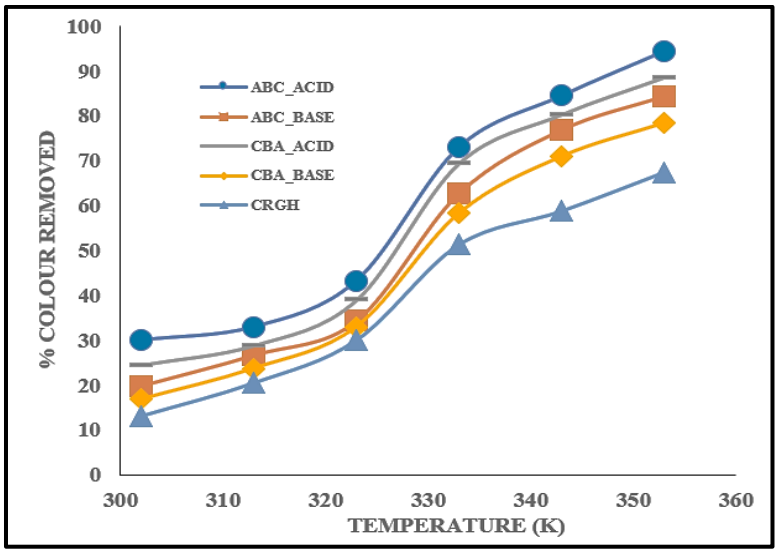

Figure 5: Effect of temperature on the adsorption efficiency

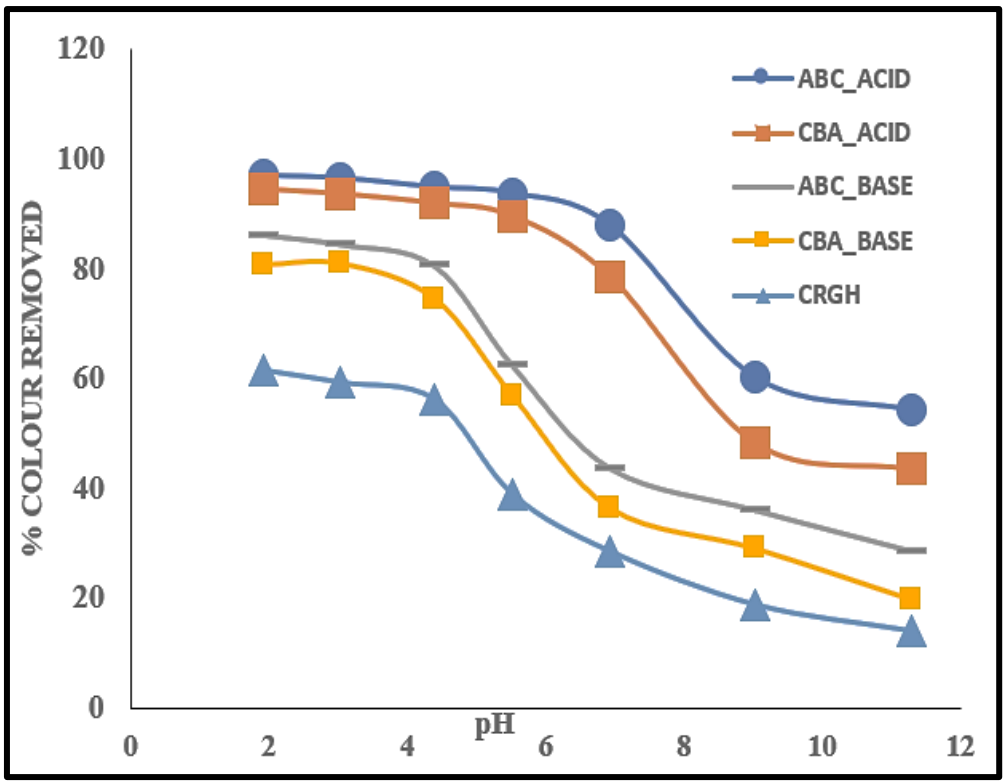

Figure 6: Effect of initial pH of solution on the adsorption efficiency

ISSN 0795 - 22066

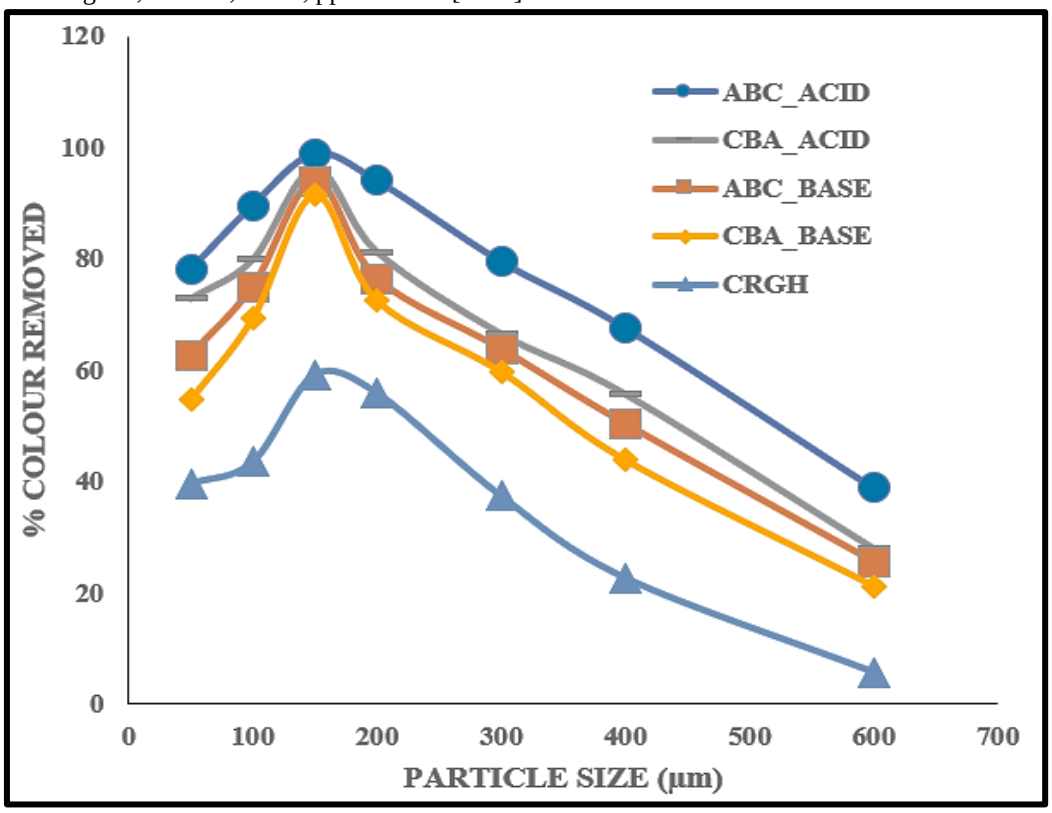

Figure 7: Effect of particle size on the adsorption efficiency

Kinetic Studies: The curves for the adsorption kinetics were obtained with ABC-ACID adsorbent at pH of 2.5, with different initial dye concentrations (100, 200 and 300 mg L^{-1}), as shown in Fig. 9. It was observed that more than 50% saturation was achieved within the first 10 minutes for the turmeric dye. Thereafter, the adsorption rate noticeably decreased, as the equilibrium was attained at about 30 minutes. Also, increase in the initial dye concentration caused an increase in the adsorption capacity.

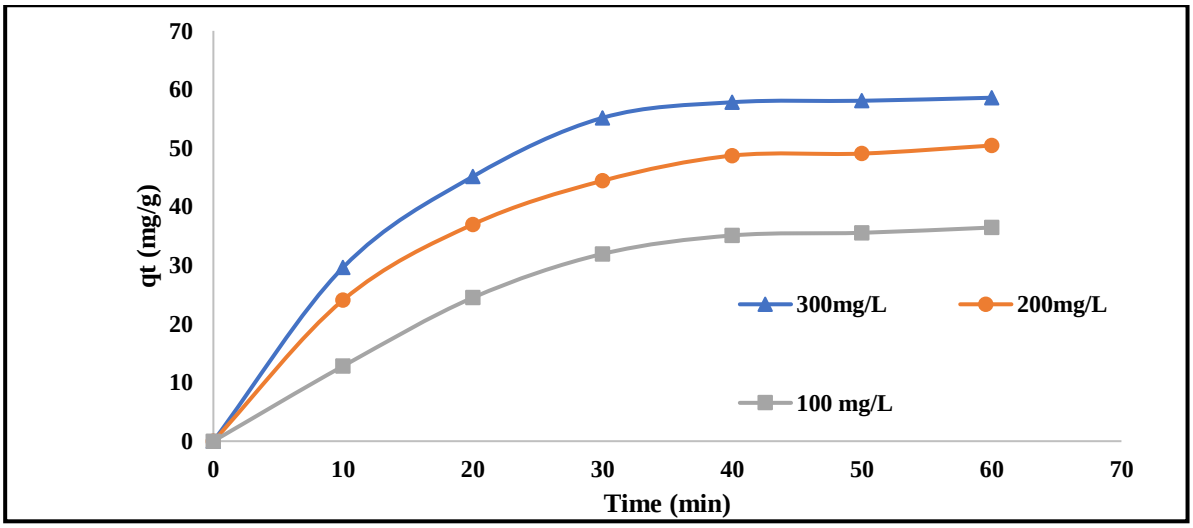

Fig. 8: Kinetic curves for the adsorption on ABC-ACID adsorbent (29 ^{0}C, 120 rpm, V = 30 mL, m = 0.1 g and pH 2.5).

ISSN 0795 - 22066

This is because more adsorption sites are occupied by the dye molecules at higher dye concentrations, leading to higher concentration gradient between bulk dye solution and surface of the adsorbent [26].As observed in Table 2, the pseudo-second order kinetic model with the highest coefficient of correlation (R^2) value of 0.9996 is most suited to the experimental data than the pseudo-first order and Elovich models (0.9648 and 0.9784 respectively). Thus, the pseudo second order kinetics best describes the interaction between the AC samples and curcumin from turmeric solution. Furthermore, the calculated q_e value from the pseudo-second order model (13.9 mg/g) is consistent with the experimental results (14.8 mg/g). This implies that the adsorption system under investigation follows a pseudo-second order kinetic model.

These results reveal that the magnitude of adsorption may be due to the higher driving force causing fast transfer of curcumin molecules to the surface of the AC samples and the availability of the uncovered surface area and the remaining active sites on the AC samples [20]. The plot for the intraparticle diffusion model has a higher regression coefficient (0.9793) than the liquid film diffusion plot (0.9648), and the intercept is not equal to zero (Table 2), so it is doubtful that intraparticle diffusion was the only rate-limiting step; hence the inference that the kinetics was regulated by both liquid film and intraparticle diffusion concurrently, though the intraparticle diffusion may have contributed more to the kinetics than the liquid film diffusion.

Table 2: Kinetic parameters for the adsorption of turmeric solution on ABC-ACID

Kinetic Model		**Parameters**
1	**Pseudo First Order**	
	q_1 (mg/g)	3.5152
	k_1 (m^{-1})	0.222
	R^2	0.9648
2	**Pseudo Second Order**	
	q_2 (mg/g)	13.09
	k_2 (m^{-1})	4.6069×10^{-3}
	q_e (mg/g) (exp)	14.8
	R^2	0.9996
3	**Elovich Equation**	
	a (mg g^{-1} min^{-1})	1.897×10^6
	b (g mg^{-1})	1.39
	R^2	0.9784
4	**Intraparticle diffusion**	
	k_i (mg g−1 $min^{-1/2}$)	0.4203
	C	10.671
	R^2	0.9793
5	**Liquid film diffusion**	
	k_{fd}	0.0222
	C	1.4375
	R^2	0.9648

***Adsorption Isotherms*:** In order to determine the suitability of the ABC-ACID adsorbent sample for turmeric dye removal, its equilibrium adsorption behaviour was studied at pH of 2.5 and dye concentration range from 25 to 350 mg L^{-1}, and the results obtained displayed on Figure 9.

ISSN 0795 - 22066

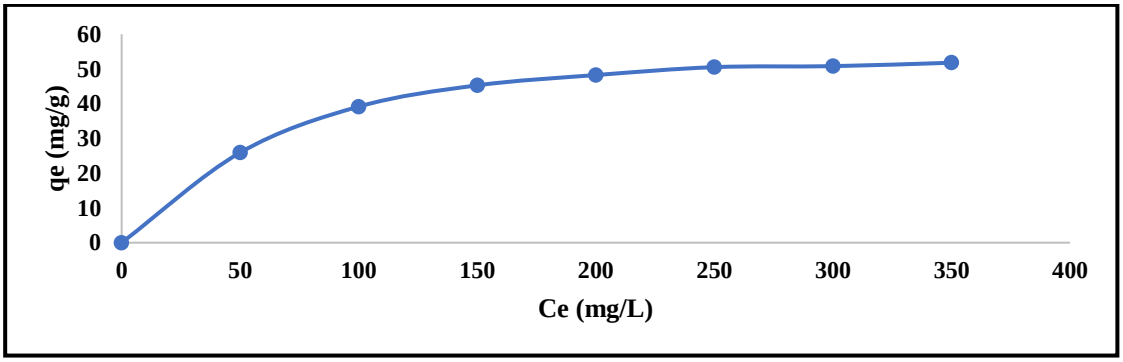

Fig. 9: Equilibrium curve for the adsorption of turmeric dye on ABC-ACID adsorbent (29 ^{0}C, 100 rpm, V = 30 mL, m = 0.1 g and pH 2.5).

It can be seen that the adsorption isotherm showed an initial curving before levelling off to a plateau. The curvature at the beginning confirms that there's a high affinity between ABC-ACID adsorbent and turmeric dye, and the plateau signifies the maximum adsorption capacity of the adsorbent. More information about the adsorption isotherms of turmeric dye on ABC-ACID adsorbent was obtained from the Freundlich, Langmiur, Temkin, and Dubinin–Radushkevich isotherms into which the experimental data were fit. The higher R^2 value obtained for the Langmiur isotherm (Table 3) established that this model gives the most suitable explanation for the adsorption equilibrium of turmeric dye onto ABC-ACID adsorbent.

An adsorption process is regarded as favourable if the Langmuir isotherm's R_L value, which is an important parameter of the Langmuir isotherm, is between 0 and 1. In this study, the R_L value is between 0 and 1, indicating that the sorption process is favourable.

The uptake of turmeric dye onto ABC-ACID was physical in nature since the adsorption energy as calculated from the DR model is not up to 8KJ/mole.

Table 3: Equilibrium data for the adsorption of turmeric dye on ABC-ACID

Model		**parameter**
1	**Freundlich**	
	K_F	33.20
	n	6.15
	R^2	0.8227
2	**Langmiur**	
	X_m (mg g^{-1})	450.45
	K_L	4.44
	R_L	0.000643
	R^2	0.9459
3	**Tempkin**	
	b_T	12, 771.25
	K_T	$1.97x10^{-18}$
	R^2	0.9395
4	**DR**	
	β	8×10^{-09}
	q_m (mg g^{-1})	52.16
	E Kj/mol	5.59
	R^2	0.9533

ISSN 0795 - 22066

CONCLUSION

In this work, two methods were employed in the preparation of four carbonaceous adsorbents from groundnut husks, while keeping the unactivated carbonaceous material as control. These five samples were characterized and used as adsorbents for the removal of a of the yellow dye from aqueous solution of turmeric. The effect of pH, temperature and particle size on the adsorption capacity of the adsorbents were studied, the kinetic studies of the adsorption were done using the pseudo first-order, second order and Elovich kinetic models, and the Freundlich, Langmiur, Tempkin and Dubinin–Radushkevich adsorption isotherm models were employed in studying the adsorption equilibrium. The results from the adsorption studies showed promising removal efficiency for the organic dye in turmeric. The activated carbon exhibited a high adsorption capacity, effectively reducing the concentration of the dye in the solution.

REFERENCES

1. Nair, K. P. (2019). Turmeric (*Curcuma longa L.)* and Ginger (Zingiber officinale Rosc.) - World's Invaluable Medicinal Spices. Switzerland: *Springer Nature*. doi:https://doi.org/10.1007/978-3-030-29189-1.

2. Oyemitan, A. I., Elusiyan, A. C., Onifade, O. A., Akanmu, A. M., Oyedeji, O. A., & McDonald, G. A. (2017). Neuropharmacological Profile and Chemical Analysis of Fresh Rhizome Essential Oil of Curcuma longa (Turmeric) Cultivated in Southwest Nigeria. *Toxicology Reports*. doi:http://dx.doi.org/10.1016/j.toxrep.2017.07.001.

3. Aggarwal, B. B., Sundaram, C., Malani, N., & Ichikawa, H. (2007). Curcumin: The Indian Solid Gold. (B. B. Aggarwal, Y. J. Surh, & S. Shishodia, Eds.) *Advances in Experimental Medicine and Biology, 595*, 1 - 75. doi:https://doi.org/10.1007/978-387-46401-5_1.

4. Nwaekpe, J. O., Anyaegbunam, H. N., Okoye, B. C., & Asumugha, G. N. (2015). Promotion of Turmeric for the Food/Pharmaceutical Industry in Nigeri. (M. M. Felipe, Ed.) *American Journal of Experimental Agriculture, 8*(6), 335-341. doi:10.9734/AJEA/2015/16517.

5. Hima , G., & Kaliaperumal , K. (2018). Turmeric: A condiment, cosmetic and cure. *Indian Journal of Dermatology, Venereology and Leprology, 84*(1), 16-21. doi:10.4103/ijdvl.IJDVL_1143_16.

6. Leonel, M., Sarmento, B. S., & Cereda, P. M. (2003). New starches for the food industry: Curcuma longa and Curcuma zedoaria. *Carbohydrate Polymers, 54*(3), 385-388. doi:https://doi.org/10.1016/S0144-8617(03)00179-6.

7. Dhanalakshmi , K., Jaganmohan , R., & Suvendu , B. (2011). Turmeric Powder and Starch: Selected Physical, Physicochemical, and Microstructural Properties. *Journal of Food Science, 76*(9), 1284 -1291. doi:10.1111/j.1750-3841.2011.02403.x

8. Hung, P. V., & Duyen, V. N. (2016). Structure, Physicochemical Characteristics and Functional Properties of Starches Isolated from Yellow (Curcuma longa) and Black (Curcuma caesia) Turmeric Rhizomes. *Starch*, 1 - 27. doi:https://doi.org/10.1002/star.201600285

ISSN 0795 - 22066

9. Maniglia , B. C., Thamiris , M. G., & Tapia-Blácido, D. R. (2022). Starch isolation from turmeric dye extraction residue and its application in active film production. *International Journal of Biological Macromolecules*, 508-519. doi:https://doi.org/10.1016/j.ijbiomac.2021.12.145.

10. Hossain, D. K., Pervez, M. F., Mia M, N. H., Mortuza, A. A., Rahaman, M. S., Karim, M. R., . . . Khan , M. A. (2017). Effect of Dye Extracting Solvents and Sensitization Time on Photovoltaic Performance of Natural Dye Sensitized Solar Cells. *Results in Physics*. doi: http://dx.doi.org/10.1016/j.rinp.2017.04.011

11. Samanchandra, A. R., Tharanga, D., & Sewvandi, G. A. (2017). Fabrication of Dye Sensitized Solar Cells using Locally Available Sensitizers. *Moratuwa Engineering Research Conference (MERCon)*, 390 - 394. doi:10.1109/MERCon.2017.7980516

12. Hossain, M., Pervez, M., Uddin, M., Tayyaba, S., Mia, M. N., Bashar, M. S., . . . Hakim, M. A. (2018). Influence of Natural Dye Adsorption on the Structural, Morphological and Optical Properties of TiO2 Based Photoanode of Dye-Sensitized Solar Cell. *Materials Science-Poland*, *36*(1), 93 - 101. doi:https://doi.org/10.1515/msp-2017-0090

13. Ruhane, T. A., Islam, T. M., Rahaman, S. M., Bhuiyan, M. M., Islam, M. M., K, N. M., . . . Khan, A. M. (2017). Photo Current Enhancement of Natural Dye Sensitized Solar Cell by Optimizing Dye Extraction and its Loading Period. *OPtik*, *149* , 174-183. doi:https://doi.org/10.1016/j.ijleo.2017.09.024

14. Syafinar, R., Gomesh, N., Irwanto, M., Fareq, M., & Irwan, Y. M. (2015). Potential of Purple Cabbage, Coffee, Blueberry and Turmeric as Nature Based Dyes for Sensitized Solar Cell (DSSC). *EnErgy Procedia*, *79*, 799-807. doi:https://doi.org/10.1016/j.egypro.2015.11.569

15. Kermit, W., Hong, Y., Chung, W. S., & Wayne, E. M. (2006). Select metal adsorption by activated carbon made from peanut shells. *Bioresource Technology*, *97*, 2266 - 2270. doi:doi:10.1016/j.biortech.2005.10.043

16. Girgis, B. S., Yunis, S. S., & Soliman, A. M. (2002). Characteristics of Activated Carbon from Peanut Hulls in Relation to Conditions of Preparation. *Materials Letters*, 164–172.

17. Den, S., Hu, B., Chen , T., Wang , B., Huang , J., Wang , Y., & Yu, G. (2015). Activated carbons prepared from peanut shell and sunflower seed shell for high CO2 adsorption. *Adsorption*. doi:10.1007/s10450-015-9655-y

18. Geeta, K., Bhavin, S., & Sanjib, K. K. (2020). Synthesis of Activated Carbon from Groundnut Shell Via Chemical Activation. *Journal of Institution of Engineers India Series E*. doi:https://doi.org/10.1007/s40034-020-00176-z

19. Ajala, L., & Ali, E. (2020, December 26). Preparation and Characterization of Groundnut Shell-Based Activated Charcoal. *Journal of Applied Science Environtal Management*, *24*(12), 2139-2146. doi:https://dx.doi.org/10.4314/jasem.v24i12.20

20. Jordana, G., Guilherme, L. D., Marcio, A. M., & Edson, L. F. (2016). Preparation of Activated Carbon from

ISSN 0795 - 22066

Peanut Shell by Conventional pyrolysis and microwave irradiation-Pyrolysis to Remove Organic Dyes. *Journal of Environmental Chemical Engineering, 4*, 266–275. doi:http://dx.doi.org/10.1016/j.jece.2015.11.018

21. Ajeigbe, H. A., Waliyar, F., Echekwu, C. A., Kunihya, A., Motagi, B. N., Eniaiyeju, D., & Inuwa, A. (2015). *A Farmer's Guide to Profitable Groundnut Production in Nigeria.* Telangana, india: International Crops Research Institute for the Semi-Arid Tropics. Retrieved from http://oar.icrisat.org/id/eprint/8856

22. Ani, D. P., Umeh, J. C., & Weye, E. A. (2013). Profitability and Economic Efficiency of Groundnut Production in Benue State, Nigeria. *African Journal of Food, Agriculture, Nutrition and Development*, 8091-8105. doi:10.18697/ajfand.59.10975

23. Seltene, A., Hussein, S., Pasupuleti, J., & Jacob, M. (2019). Groundnut (Arachis hypogaea L.) Improvement in Sub-Saharan Africa: a Review. *Acta Agriculturae Scandinavica, Section B-Soil and Plant Science , 69*(6), 528-545. doi:10.1080/09064710.2019.1601252

24. Nady, A. F., Sohair, A. S., & Reham, M. M.-e. (2012). Effect of Activation Temperature on Textural and Adsorptive Properties for Activated Carbon Derived from Local Reed Biomass: Removal of pNitrophenol. *Environmental research, Engineering and Management, 59*(1).

25. Kalyani, p., & Anitha, A. (2013). Refuse Derived Energy - Tea Derived Boric Acid Activated. *Portugaliae Electrochimica Acta, 31*(3), 165-174. doi:DOI: 10.4152/pea.201303165

26. Soumia, B., Zahra, S., Nabil, B., Brahim, S., Ouiza, A., Devouge-Boyer, C., . . . Vieillard, J. (2022). Functional activated carbon: from synthesis to groundwater fluoride removal†. *RSC Advances, 12*, 2332 - 2348. doi:10.1039/d1ra08209d

27. Suzhen, B., Tiantian, W., Tian, Kesheng, c., & Jitao, L. (2020). Facile Preparation of Porous Biomass Charcoal from Peanut Shell as Adsorbent. *Scientific ReportS, 10*. doi:https://doi.org/10.1038/s41598-020-72721-0

ISSN 0795 - 22066